analytical chemistry

Article

pubs.acs.org/ac

Laser Desorption Ionization Mass Spectrometry Imaging of *Drosophila* Brain Using Matrix Sublimation versus Modification with Nanoparticles

Nhu T. N. Phan,[†,‡] Amir Saeid Mohammadi,[‡,§] Masoumeh Dowlatshahi Pour,[‡,§] and Andrew G. Ewing*[,†,‡,§]

[†]Department of Chemistry and Molecular Biology, University of Gothenburg, Kemivägen 10, SE-412 96 Gothenburg, Sweden

[‡]National Center Imaging Mass Spectrometry, Kemivägen 10, SE-412 96 Gothenburg, Sweden

[§]Department of Chemical and Biological Engineering, Chalmers University of Technology, Kemivägen 10, SE-412 96 Gothenburg, Sweden

Supporting Information

ABSTRACT: Laser desorption ionization mass spectrometry (LDI-MS) is used to image brain lipids in the fruit fly, *Drosophila*, a common invertebrate model organism in biological and neurological studies. Three different sample preparation methods, including sublimation with two common organic matrixes for matrix-assisted laser desorption ionization (MALDI) and surface-assisted laser desorption ionization (SALDI) using gold nanoparticles, are examined for sample profiling and imaging the fly brain. Recrystallization with trifluoroacetic acid following matrix deposition in MALDI is shown to increase the incorporation of biomolecules with one matrix, resulting in more efficient ionization, but not for the other matrix. The key finding here is that the mass fragments observed for the fly brain slices with different surface modifications are significantly different. Thus, these approaches can be combined to provide complementary analysis of chemical composition, particularly for the small metabolites, diacylglycerides, phosphatidylcholines, and triacylglycerides, in the fly brain. Furthermore, imaging appears to be beneficial using modification with gold nanoparticles in place of matrix in this application showing its potential for cellular and subcellular imaging. The imaging protocol developed here with both MALDI and SALDI provides the best and most diverse lipid chemical images of the fly brain to date with LDI.

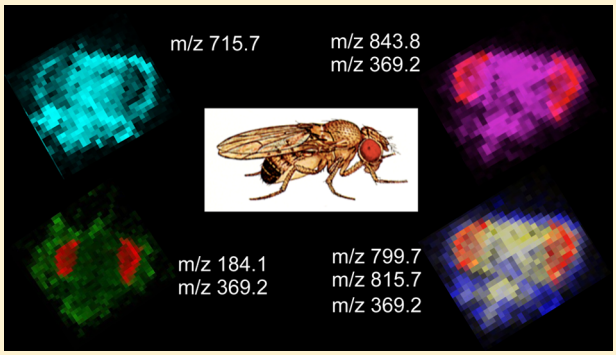

The fruit fly, *Drosophila melanogaster*, is one of the most common invertebrate model organisms in biological and neurological research owing to its important features relevant to mammalian systems. The most important aspect is that, although having a simple genome comprising 14 000 genes, the fly has functional orthologs to over 60% of human genes. Molecular mechanisms such as metabolism, organogenesis, and neural development in flies are conserved. The wide range of complex behaviors in flies, for instance, learning and memory, sleep, courtship, drug addiction, etc., are relevant to human and other mammalian organisms. In addition, a short lifetime in flies (typically about 2 weeks at 20−25 °C) facilitates experimental work and statistical analysis, which requires large numbers of samples. *Drosophila* is a common model in genetic studies and research on brain disorders, particularly Parkinson's disease, epilepsy, and Niemann−Pick disease.[1−4] Whole *Drosophila* and their egg chambers have been imaged with laser desorption methods in mass spectrometry.[5,6] More recently, *Drosophila* has also been used to study drug addiction and, recently with liquid chromatography and secondary ion mass spectrometry, to investigate the effects of the stimulant drug methylphenidate on both the neurotransmitter levels and the lipid structure of the fly brain.[7,8]

Matrix-assisted laser desorption ionization mass spectrometry (MALDI-MS) has been widely applied as an important imaging technique for organic compounds in biological, pharmaceutical, and medical science. The technique provides distributional information on the analytes in the mass range from several hundred to a hundred thousand daltons in which intact lipids, peptides, and proteins are detected. One of the main challenges in MALDI imaging is spatial resolution, making it difficult to extend the application of MALDI to cellular and subcellular analysis. Spatial resolution typically depends on the laser spot size and the matrix crystal size. With a given laser spot size, a homogeneous layer of matrix with very small size of matrix crystals ensures the best achievable spatial resolution. The choice of matrix and matrix deposition methods are critical factors determining the properties of the matrix layer and therefore the

Received: October 17, 2015
Accepted: December 25, 2015
Published: December 25, 2015

DOI: 10.1021/acs.analchem.5b03942
Anal. Chem. 2016, 88, 1734−1741

spatial resolution. Various matrix deposition methods have been developed including manual and automatic deposition such as the use of airbrush, sprayer, inkjet printer, and sublimation.[9,10] Sublimation, has been shown to produce very small matrix crystals and limited diffusion of the analytes compared to spraying methods. The crystal sizes of the commonly used matrixes 2,5-dihydroxybenzoic acid (DHB) and α-cyano-4-hydroxycinnamic acid (CHCA) are generally in the range from 5 to 20 μm using spraying deposition. Sublimation, however, produces matrix crystals generally from 1 to 3 μm in size.[11,12] However, due to its solvent-free mechanism, sublimation might result in poor extraction of the analytes. Recrystallization and rewetting of the sample surface after sublimation have been suggested in order to increase the extraction efficiency and sensitivity of the biomolecules.[11] Bouschen et al. deposited a sublimed DHB layer in saturated water atmosphere.[13] This provided improvement in signal intensity for biomolecules of m/z < 3000 Da in tissue and single cell samples. A similar approach has been utilized to improve detection sensitivity of proteins up to m/z 30 000 Da with different recrystallization solutions including water, water/methanol, water/acetic acid, and trifluoroacetic acid (TFA).[11]

Another challenge in MALDI is detectable mass range. Although suitable for analysis of a wide range of biomolecules, MALDI is often not easy with small molecules and metabolites owing to the dramatic interference caused by the organic matrix. Different matrixes are better for detecting different ionic species. The matrix DHB has been widely used to analyze phospholipids, peptides, and small proteins, whereas CHCA is common matrix for peptides and proteins.[14,15] Sinapinic acid, on the other hand, is mainly used for proteins.[16] A current tendency has been to use nanoparticles as an alternative material for standard organic matrix for SALDI. Nanoparticles of various materials such as iron oxide,[17] silver,[18] titanium dioxide,[19] diamond,[20] bare silica,[21] and a mixture of them[22,23] with the size ranging from 2 to 100 nm have been investigated. Among different nanoparticle materials, gold nanoparticles (AuNPs), in particular, have been increasingly used as a SALDI matrix to analyze biomolecules such as peptides, carbohydrates, glycosphingolipids, triacylglycerides.[24−26] Owing to surface plasmon resonance, AuNPs serve as an efficient reservoir for photon energy deposition as well as an energy transfer media for the analytes via the thermal propagation process, thus resulting in significantly enhanced ionization of the analytes.[27,28] In addition, the AuNP matrix offers selective ionization for some biomolecules especially triacylglycerides and glycosphingolipids, providing better selectivity compared to organic matrixes. Surface modification with inorganic or metallic nanoparticles eliminates the interferences at the low-mass range as well as potentially improving the spatial resolution to the subcellular level. Although the improved performance obtained with nanoparticles for laser desorption ionization (LDI) has been increasingly acknowledged, its applications have been still modest compared to MALDI using conventional organic matrix. The applications of nanoparticles for LDI in biological imaging can be found in the outstanding literature.[17,18,26,29−32]

In this paper, we apply both MALDI-MS and SALDI-MS to image the lipid structure of *Drosophila* brain. We have examined three different sample preparation approaches including sublimation with two common organic matrixes and surface modification with nanoparticles to increase the information we can obtain from the images. In MALDI and SALDI imaging there have been reports of differential enhancements of the triacylglycerides and other lipids by using different matrixes such as AuNPs and DHB.[25,31] We use this to enhance our images and show that TFA with one matrix enhances the signal in the MS improving the sensitivity of lipid detection, but does not with the other matrix, and this enhances the ability to image different lipids in the fly brain. We confirm that the different sample preparation methods are more suitable for detection of different biomolecules, based primarily on mass-to-charge (m/z) range, including small molecules less than 400 Da, diacylglycerides, intact lipids, and triacylglycerides in the fly brains, and these lipids distribute unevenly over the fly brain. With this combined approach, we have obtained some of the best and most diverse chemical images of the fly brain to date.

EXPERIMENTAL SECTION

Fly Brain Section Sample Preparation for MALDI Imaging. Transgenic *Drosophila* (TH-GFP) was cultured on potato meal/agar medium, and 4−7 day old male flies were selected for experiments. The protocol for sample preparation and sectioning follows previous literature.[8,33] In brief, to ensure all the flies are in the same orientation for sectioning, up to 11 flies were loaded into a fly collar (4 M Instrument & Tool LLC, U.S.A.) which was then transferred to aluminum mold. The mold was filled up with gelatin 10% (Sigma-Aldrich, Stockholm, Sweden) and then allowed to solidify and frozen at −20 °C. The frozen gelatin block containing the fly heads was detached from the fly collar and sectioned into slices of 17 μm thickness. The fly head sections were transferred to indium−tin oxide (ITO)-coated slides (Bruker Daltonics, Germany), which were subsequently freeze-dried in high vacuum (10^{-3} mbar) for 2 h. Fly brain sections were kept in millibar vacuum so that the water sublimed slowly to dryness to prevent delocalization of the biomolecules. Freeze-drying is a standard sample preparation method to preserve the morphology and chemical structure of biological tissue samples. Freeze-drying has been widely used in a number of biological applications using secondary ion mass spectrometry imaging (SIMS) and MALDI imaging.[16,34] After freeze-drying, the freeze-dried brains were ready for further matrix sublimation with either CHCA or DHB (Sigma-Aldrich, Stockholm, Sweden) or, alternatively, modified with AuNPs having ∼10 nm diameter.

Sublimation with Organic Matrix Deposition. The vacuum sublimation chamber (Sigma-Aldrich, Stockholm, Sweden) comprises an inner flat top and an outer bottom attached to each other by an O-ring-sealed flange. The chamber was coupled to a rough pump connected to a digital vacuum gauge controller and positioned on a heater. The temperature was monitored by a digital thermometer. Sublimation was performed by the following steps.

First, ITO-coated glass slides containing brain tissues were attached to the flat top of the chamber using double-sided tape. The matrix powder was spread evenly at the outer bottom of the chamber, which was then attached to the top using the O-ring seal. Vacuum was then applied, and 15 min after the pressure reduced to 0.8 mbar, the top was filled with the cold water (5 °C) for the condensation of the matrix on the sample slides. After another 5 min, heat was applied to the bottom of the chamber. The optimized conditions for sublimation of DHB and CHCA matrixes were 10 and 30 min at temperature of 145 and 200 °C, respectively, under a stable vacuum of 0.8 mbar. The heat was then removed and the chamber was allowed to cool down to room temperature.

Matrix deposition with automatic sprayer Image Prep. The Image Prep was purchased from Bruker Daltonics (Bremen,

DOI: 10.1021/acs.analchem.5b03942
Anal. Chem. 2016, 88, 1734−1741

Germany). DHB solution was prepared at a concentration of 20 g/L in 50% acetonitrile and 0.1% TFA. The matrix solution was sprayed on the sample surface using an automatic matrix preparation method for DHB, which is specified by continuous cycles of spraying for 2 s, incubation for 30 s, drying for 30 s, and safe drying for 30 s in every eighth cycle. The deposition process was monitored using the signal of scattering light from the crystalline matrix layer on sample surface. The deposition finishes when the final voltage difference (sensor voltage compared to the voltage at the beginning) reaches 0.5 V.

Nanoparticle Modification Procedure. A solution of citrate-capped 10 nm AuNPs was prepared using the citrate reduction method described by Kimling et al.[35] A 1.5 mL solution of 10 nm AuNPs was suspended in ethanol at a concentration of 0.6 mg/mL. The solution was sprayed onto the slide containing fly brain tissue from a distance of 15 cm with a flow rate of 0.75 mL/min. The distance and the flow rate are critical parameters to prevent wetting of the sample. The nanoparticles are stable forming few clusters when sprayed on the sample as observed in the distribution of AuNPs on the sample surface with scanning electron microscopy (SEM), shown in Figure S1.

Recrystallization with Trifluoroacetic Acid Treatment. After matrix sublimation in the vacuum, the brain samples were positioned next to a disk of 0.5 mL of TFA solution (99%) in a desiccator. The desiccator was then tightly sealed for 30 min during which TFA vapor was used to gently wet the matrix layer to integrate the analytes into the matrix.

MALDI-MS Imaging Instrumental Parameters. MALDI imaging was performed using a MALDI-TOF Ultraflextreme instrument (Bruker Daltonics, Bremen, Germany) equipped with a Smartbeam laser Nd:YAG/355 nm. Acquisition was obtained with a spatial resolution of 20 μm (laser focus 20 μm in diameter and raster size 20 μm). Imaging was performed in the positive ion mode with a mass range from 400 to 3500 Da for matrix sublimation with CHCA and DHB and with a mass range from 80 to 3500 for the AuNP modification. Laser energy was adjusted before analysis, which was in the range of 80−90% of the energy to obtain high signal-to-noise ratio. The spectra were acquired by a sum of 1000 shots for each raster point with a laser repetition rate of 1000 Hz. The instrument provided mass resolution of ∼15 000 at m/z 869.85. Data were acquired using FlexControl software version 3.0 (Bruker Daltonics, Germany). Image data were visualized using FlexImaging version 3.0, and spectra data were analyzed using FlexAnalysis 3.4 (Bruker Daltonics, Germany). Instrument calibration was performed every day before measurements using a standard calibration mixture of monopeptides (Bruker, Germany).

RESULTS AND DISCUSSION

Sample Preparation. Sample preparation is one of the crucial steps determining the success of imaging biological samples. This is mainly reflected in the reliability and reproducibility of the sample. In order to ensure high reliability and reproducibility, the spatial localization of the analytes on the sample must be preserved. A variety of sample preparation protocols have been developed for different imaging techniques in order to prepare a sample suitable for analysis while maintaining the original spatial distribution of the analytes on the samples.[15] For MALDI imaging of biological tissue samples, the tissues typically undergo dissection, sectioning, and are further modified with different matrix or reagents. In addition to the distribution of the analytes, tissue sections must also be reproducible among different samples. This is sometimes difficult to achieve, especially for a heterogeneous and complex biological sample such as brain tissue. In our experiments, the use of a fly collar is extremely helpful to be able to control the depth and orientation when sectioning a fly head <1 mm in length. In addition, as up to 11 heads can be loaded into the collar to be sectioned at the same time, the fly brain sections have similar depth in the brains, and this contribute to high reproducibility of the measurements. To facilitate sectioning with the fly collar, embedding material has been used to form an embedding block containing fly heads when detached from the fly collar. Two embedding materials, optimum cutting temperature (OCT) (Histolab, Sweden) and gelatin (Sigma-Aldrich, Sweden), were examined to determine which is best to obtain good brain sections by cryomicrotome sectioning and for potential interference in MS spectra. OCT is a common embedding material in histology and microscopy, whereas gelatin has been used for sectioning of fly brains[8] and breast tumors.[36] OCT provided much easier and better cutting than gelatin with well-preserved morphological structure of the brain sections; however, we find it has significant spectral interferences in the MS compared to gelatin. From the spectra of OCT (Figure S2A), very high peak clusters cover the mass range from m/z 900−2200. These peaks have been observed with LC−MS,[37] representing poly(ethylene glycol), one of the main compositions of OCT compounds, and are problematic as they cover the mass range of interest for fly brain lipids and peptides. At lower mass range, OCT peaks also partially overlap with peaks from the fly brain. The spectra of gelatin have less intense peaks scattered in the low-mass range of m/z 100−600. An overlay of the gelatin and the fly brain spectra shows less significant interference of gelatin peaks from the signals of the fly brain compared to OCT (Figure S2B). Gelatin therefore was used as embedding material for fly brain sectioning in further experiments.

Detection of Small Molecules and Lipids. We have examined the detectability of three different sample modification methods for small molecules and lipids in the fly brains by LDI imaging. Sample modification methods including sublimation with CHCA, DHB, and surface coating with AuNPs have been examined regarding the detectable mass range and spatial resolution for fly brain imaging. In order to increase the ionization efficiency for biomolecules in the brain, integration of the biomolecules into the matrix is necessary for LDI analysis. We employed the recrystallization method with TFA after matrix sublimation or nanoparticle modification to investigate its benefits for lipid imaging in our fly brain samples.

Recrystallization of the matrix, under the conditions used here, produces small crystal sizes,[38] and these can be smaller than 1 μm.[12] Figure 1 compares the spectra obtained from the fly brains with and without TFA treatment on both DHB and CHCA matrix. With the DHB matrix, signal intensities of ion species between 500 and 850 Da are increased about 2-fold in the TFA-treated fly brains compared to TFA-free samples. The peaks with enhanced signal intensity on a fly brain sublimated with DHB and treated with TFA are listed on Table S1. With the CHCA matrix, however, TFA insignificantly affects the sensitivity of the analytes. In addition, there are differences in the detected molecules between the DHB and CHCA matrixes. In particular, significantly high signals of molecules above 800 Da are obtained in the spectra of DHB sublimation, whereas very small peaks are detected using CHCA. The mechanism for this effect is not clearly understood; however, it is clear that DHB is more effective for high-mass lipids, whereas CHCA is favorable

DOI: 10.1021/acs.analchem.5b03942
Anal. Chem. 2016, 88, 1734−1741

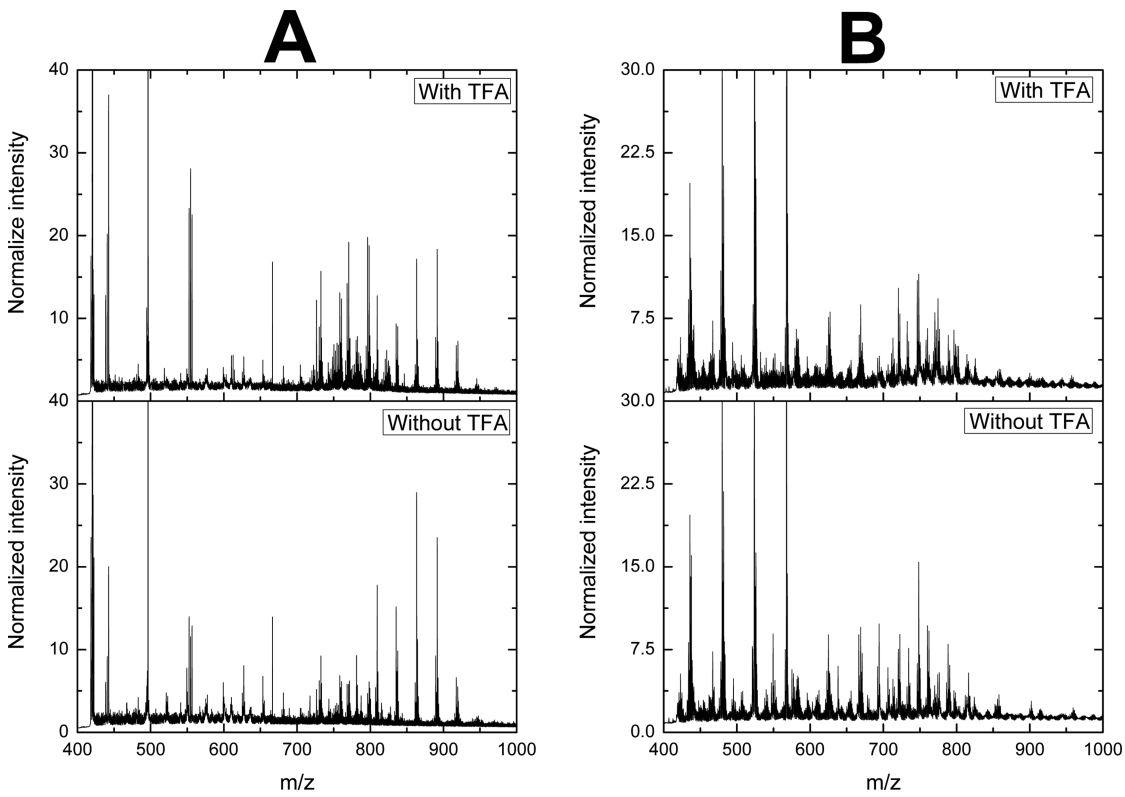

Figure 1. Representative spectra of the fly brain in positive mode with and without TFA modification. (A) Sublimation with matrix DHB. (B) Sublimation with matrix α-CHCA. Spatial resolution is 20 μm.

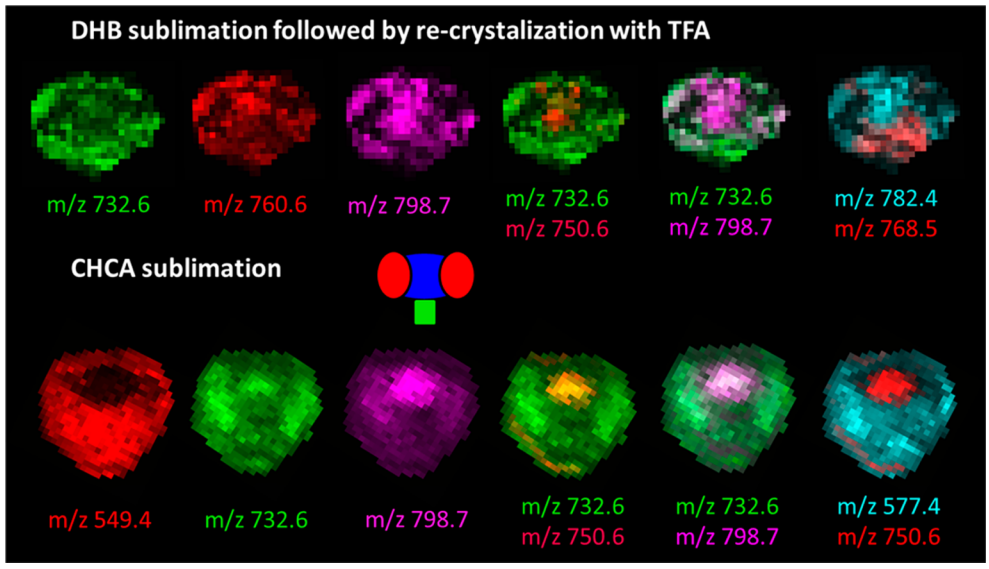

Figure 2. MALDI ion images of the fly brains sublimed with DHB and CHCA show different lipids detected: DAG (32:1) at m/z 549.4, DAG (34:1) at m/z 577.4, PC (32:1) at m/z 732.6; PC (34:1) at m/z 760.6, $[SP(C18:0) + Na]^+$ at m/z 750.6, PE (38:4) at m/z 768.5, PC (36:4) at m/z 782.4, and $[PC (34:1) + K]^+$ at m/z 798.7. All images were acquired with spatial resolution of 20 μm as defined by the beam size and raster size. Symbolic figure on the top shows the orientation of the fly brain: the two red parts on the side are optical lobes, the central brain is in the middle (blue), and the lower part is the proboscis (green).

for detection of low-mass lipids and metabolites in these brain slices. On the basis of these results, sublimation with DHB followed by TFA modification and sublimation with CHCA have been further used for fly brain imaging.

Ion images of the fly brains obtained by MALDI imaging with spatial resolution (beam size and raster size) 20 μm are shown in Figure 2. Different molecules clearly distribute differently across the fly brain. For sublimation with DHB followed by TFA modification, the lipid PC (32:1) at m/z 732.6 distributes across the whole brain but is more intense in the optical lobes while the lipid PC (34:1) at m/z 760.6 localizes at higher intensity in the central brain and optical lobes. The salt adduct $[PC (34:1) + K]^+$

DOI: 10.1021/acs.analchem.5b03942
Anal. Chem. 2016, 88, 1734−1741

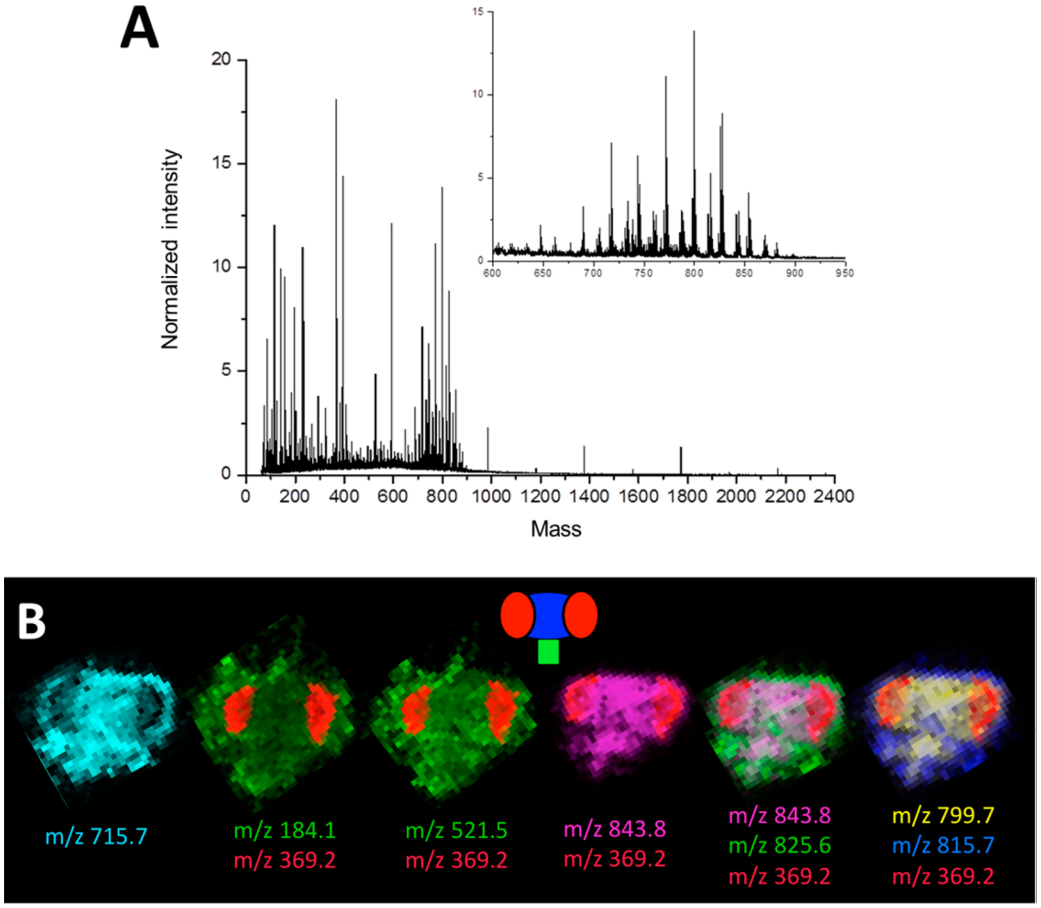

Figure 3. Spectra and ion images of small molecules and triacylglycerides on the fly brain using AuNPs as surface modification for SALDI. Spatial resolution is 20 μm as defined by the beam size and raster size. (A) Spectra. (B) Ion image. PC headgroup at m/z 184.1, drosopterin at m/z 369.2, DAG (30:1) at m/z 521.5, TAG (42:4) at m/z 715.7, $[TAG (46:1) + Na]^+$ at m/z 799.7, $[TAG (49:0) + Na]^+$ at m/z 843.8, TAG (49:3) at m/z 815.7, and $[TAG (48:2) + Na]^+$ at m/z 825.6. Symbolic figure on the top shows the orientation of the fly brain: the two red parts on the side are optical lobes, the central brain is in the middle (blue), and the lower part is the proboscis (green).

at m/z 798.7 exhibits similar localization with its molecular lipid PC (34:1). An overlay of different ion images shows that several biomolecules have distinct localizations. The glycosphingolipid $[SP(C18:0) + Na]^+$ at m/z 750.6 mainly localizes in the central brain. Phosphatidylethanolamine PE (38:4), at m/z 768.5, is more intense in the proboscis, whereas a high level of PC (36:4) at m/z 782.4 is found in the central brain and optical lobes. For CHCA sublimation, low-mass species can be detected such as diacylglyceride DAG (32:1) at m/z 549.4 and DAG (34:1) at m/z 577.4, which are found in the optical lobes and proboscis. In addition, several lipids that are detected by both DHB and CHCA sublimation, for example PC (32:1), $[PC (34:1) + K]^+$, and $[SP(C18:0) + Na]^+$, show good correlation in their distributions for the two preparations schemes. With 20 μm spatial resolution, the matrix crystals are sufficiently small to provide information about the distribution of biomolecules in different regions of the fly brain section such as the central brain, optical lobes, and proboscis which have typical sizes about 300−400 μm, 200 μm each, and 300 μm, respectively.

Gold Nanoparticles as Matrix. Sample modification with nanoparticles has been applied as an alternative to standard organic matrix to carry out what is typically called SALDI-MS with several apparent advantages.[17,27] The ionization process occurs thermally, which results in fewer spectral interferences, and therefore the detectable mass range can be extended to lower than 400 Da, which is the usual limit for organic matrix materials. To exemplify this issue, Figures S3 and S4 show the spectral interferences of matrix DHB and CHCA at mass range lower than 400 Da. The NP matrix also eliminates the formation of heterogeneous matrix crystals offering high spatial resolution for imaging and is independent of the irradiation wavelength. Therefore, we applied AuNPs as a matrix for laser desorption to carry out profiling and imaging of the fly brain with the aim to compare the ionization capability and detectability for biomolecules in fly brains with conventional organic matrix materials.

In order to obtain the highest performance of AuNPs as a matrix for fly brain analysis, a homogeneous coverage of AuNPs on the sample surface is a critical requirement so that it produces even ionization across the entire sample area. This is achieved by spraying the AuNPs as a solution in ethanol with an airbrush. The coverage of AuNPs on the fly brain was examined with SEM (Figure S5). The AuNPs distributed homogeneously on the surface of the eye—the area on the edge of the brain with topographic features—and the central part of the fly brain.

Spectra from the fly brain analyzed following AuNP deposition (Figure 3A) show a high signal for small ionic species with mass $m/z < 400$ Da. For this mass range, several biologically important species in the fly brain, particularly the common headgroup fragment of the lipid phosphatidylcholine at m/z 184.1, the eye pigment drosopterin at m/z 369.2,[33] and DAGs, are clearly observed in the spectra. In addition, high-mass molecules

DOI: 10.1021/acs.analchem.5b03942
Anal. Chem. 2016, 88, 1734−1741

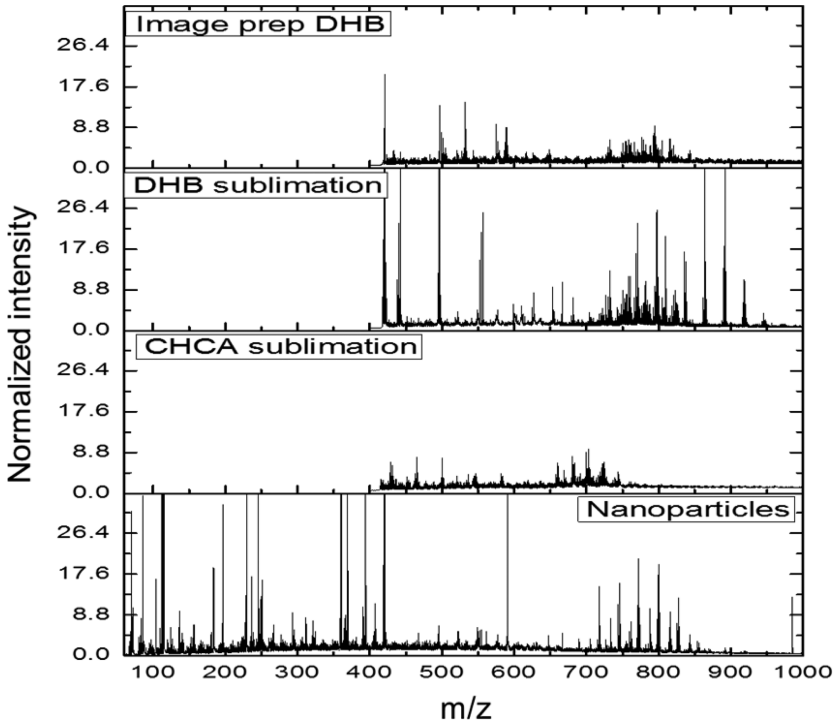

Figure 4. Comparison of MALDI and SALDI spectra for fly brains obtained from different sample preparation methods in positive mode: Image Prep automatic spraying with DHB, sublimation with DHB followed by recrystallization with TFA, sublimation with CHCA, and modification with AuNPs.

especially triacylglycerides (TAGs) and their salt adducts with potassium having m/z up to 1000 Da are observed. Intact PCs are not observed but more likely to be fragmented to smaller fragments with the typical ions at m/z 86.1 and PC headgroup m/z 184.1. This was confirmed by analysis of the lipid standards DLPC at m/z 782.4 and DOPC at m/z 786.5 at concentrations of 100 and 250 μg/mL, respectively (Figures S6–S8). In addition, no or insignificant peaks are detected above m/z 1000 Da, except for Au cluster peaks. The experiment using TFA modification on a AuNP matrix has also been performed; however, the result is not different compared to that without TFA.

For imaging fly brain using AuNPs, the laser diameter and raster size of 20 μm, which produces a minimum spatial resolution of 20 μm, has been used in a similar manner to the experiments described for imaging with sublimation. Use of the AuNP matrix provides visually better resolution ion images of the eyes, optical lobes, central brain, and proboscis despite the same laser spot size. Figure 3B shows the distributions of specific molecules in a fly brain following deposition of AuNPs. The ion image of TAG (42:4) at m/z 715.7 shows its distribution across the fly brain and clearly shows the empty eye area. The overlay of ion images between the eye pigment drosopterin at m/z 369.2 and other ion species is also presented. The PC fragment at m/z 184.1 distributes in the entire fly brain, which is similar to DAG (32:1) at m/z 521.5. The fragments $[TAG\ (49:0) + Na]^+$ at m/z 843.8, TAG (47:3) at m/z 787.7, and $[TAG\ (46:1) + Na]^+$ at m/z 799.7 are predominantly present in the central brain and optical lobes, whereas $[TAG\ (44:1) + Na]^+$ at m/z 771.6, TAG (49:3) at m/z 815.7, and $[TAG\ (48:2) + Na]^+$ at m/z 825.6 distribute in the entire brain including the cuticle and proboscis.

It is clear that the use of AuNPs as matrix extends the detectable mass range to below 400 Da for small molecular fragments and molecules and appears to provide better ion images compared to DHB and CHCA matrixes. Biomolecules, however, are detected differently using these three materials, as each is favorable to a specific mass range or groups of molecules, and this is discussed next.

Analytical Performance Comparison of Sample Modification Techniques for MALDI and SALDI Imaging of Fly Brain. Among different matrix deposition methods, in terms of detection mass range, it is clearly evident that the AuNP matrix is beneficial for detection of low-mass species, especially below m/z 400 Da. Figure 4 compares the spectra from fly brains obtained by LDI following different sample preparation methods. What is interesting is that different sample preparation methods lead to the detection of different biomolecules. Sublimation with DHB tends to lead to detection of higher-mass PC lipids (approximately m/z 700–850 Da) compared to sublimation with CHCA (approximately m/z 550–750 Da). AuNP modification, however, leads to detection of small molecules, molecular lipids such as diacylglycerides, and triacylglycerides up to m/z 850 Da. In addition, sublimation together with TFA treatment and automatic spraying were compared using the same matrix material DHB. The sublimation with TFA treatment produces peaks with intensity more than 2 times higher compared to those obtained by automatic spraying. This explains the narrower detectable mass range using the automatic spraying method. The low sensitivity of the matrix spraying method results from the heterogeneous formation of large matrix crystals during the spraying process, which decreases the ionization efficiency of the biomolecules.

Above m/z 1000 Da, DHB and CHCA matrix sublimation both allow detection of lipid dimers, at about m/z 1500 Da for DHB and m/z 1300 and 1800 Da for CHCA, however, at very low intensity. In contrast, there are no peaks detected at the range above 1000 Da using AuNPs, except the peaks for Au clusters (Figure S9). This might result from a large amount of small molecules, particularly salts and lipids, being present on the sample surface, which causes signal suppression for large molecules in this mass range.

DOI: 10.1021/acs.analchem.5b03942
Anal. Chem. 2016, 88, 1734–1741

Table 1. MS Peaks Detected for Fly Brains Using Different Sample Preparation Methods

	DHB	CHCA	NPs	peak assignment
small molecules and DAG $[M + H]^+$			184.1	PC fragment $C_5H_{15}NPO_4^+$
			369.2	drosopterin $[C_{15}H_{16}O_2N_{10} + H]^+$
			521.5	DAG (30:1) $C_{33}H_{61}O_4^+$
			523.5	DAG (30:0) $C_{33}H_{63}O_4^+$
		549.4	549.4	DAG (32:1) $C_{35}H_{65}O_4^+$
		577.4	577.4	DAG (34:1) $C_{37}H_{69}O_4^+$
glycosphingolipids $[M + Na]^+$		746.6		$[SP(C18:2) + Na]^+$ $C_{42}H_{77}NO_8Na^+$
		748.6		$[SP(C18:1) + Na]^+$ $C_{42}H_{79}NO_8Na^+$
	750.6	750.6		$[SP(C18:0) + Na]^+$ $C_{42}H_{81}NO_8Na^+$
PC $[M + H]^+$	730.5			PC (32:2) $C_{40}H_{77}NO_8P^+$
	732.6	732.6		PC (32:1) $C_{40}H_{79}NO_8P^+$
	758.6			PC (34:2) $C_{42}H_{81}NO_8P^+$
	760.6			PC (34:1) $C_{42}H_{83}NO_8P^+$
	782.4			PC (36:4) $C_{44}H_{81}NO_8P^+$
$[PC + K]^+$	796.6			$[PC (34:2) + K]^+$ $C_{42}H_{80}NO_8PK^+$
	798.7	798.7		$[PC (34:1) + K]^+$ $C_{42}H_{82}NO_8PK^+$
	820.6			$[PC (36:4) + K]^+$ $C_{44}H_{80}NO_8PK^+$
	822.6			$[PC (36:3) + K]^+$ $C_{44}H_{82}NO_8PK^+$
	824.6			$[PC (36:2) + K]^+$ $C_{44}H_{84}NO_8PK^+$
PE $[PE + H]^+$	766.6			PE (38:5) $C_{43}H_{77}NO_8P^+$
	768.5			PE (38:4) $C_{43}H_{79}NO_8P^+$
	770.6	770.6		PE (38:3) $C_{43}H_{81}NO_8P^+$
	772.6	772.6		PE (38:2) $C_{43}H_{83}NO_8P^+$
		774.6		PE (38:1) $C_{43}H_{85}NO_8P^+$
TAG $[M + H]^+$/TAG $[M + Na]^+$			715.7	TAG (42:4) $C_{45}H_{79}O_6^+$ or $[TAG (40:1) + Na]^+$ $C_{43}H_{80}O_6Na^+$
			717.7	TAG (42:3) $C_{45}H_{81}O_6^+$ or $[TAG (40:0) + Na]^+$ $C_{43}H_{82}O_6Na^+$
			759.7	TAG (45:2) $C_{48}H_{87}O_6^+$ or $[TAG (43:0) + Na]^+$ $C_{46}H_{88}O_6Na^+$
			787.7	TAG (47:3) $C_{50}H_{91}O_6^+$ or $[TAG (45:0) + Na]^+$ $C_{48}H_{92}O_6Na^+$
			815.7	TAG (49:3) $C_{52}H_{95}O_6^+$ or $[TAG (47:0) + Na]^+$ $C_{50}H_{96}O_6Na^+$
			743.6	TAG (44:4) $C_{47}H_{83}O_6^+$ or $[TAG (42:1) + Na]^+$ $C_{45}H_{84}O_6Na^+$
			745.6	TAG (44:3) $C_{47}H_{85}O_6^+$ or $[TAG (42:0) + Na]^+$ $C_{45}H_{86}O_6Na^+$
			769.7	TAG (46:5) $C_{49}H_{85}O_6^+$ or $[TAG (44:2) + Na]^+$ $C_{47}H_{86}O_6Na^+$
			771.6	TAG (46:4) $C_{49}H_{87}O_6^+$ or $[TAG (44:1) + Na]^+$ $C_{47}H_{88}O_6Na^+$
			773.7	TAG (46:3) $C_{49}H_{89}O_6^+$ or $[TAG (44:0) + Na]^+$ $C_{47}H_{90}O_6Na^+$
			797.7	TAG (48:5) $C_{51}H_{89}O_6^+$ or $[TAG (46:2) + Na]^+$ $C_{49}H_{90}O_6Na^+$
			799.7	TAG (48:4) $C_{51}H_{91}O_6^+$ or $[TAG (46:1) + Na]^+$ $C_{49}H_{92}O_6Na^+$
			825.6	TAG (50:5) $C_{53}H_{93}O_6^+$ or $[TAG (48:2) + Na]^+$ $C_{51}H_{94}O_6Na^+$
			827.7	TAG (50:4) $C_{53}H_{95}O_6^+$ or $[TAG (48:1) + Na]^+$ $C_{51}H_{96}O_6Na^+$
			841.7	TAG (51:4) $C_{54}H_{97}O_6^+$ or $[TAG (49:1) + Na]^+$ $C_{52}H_{98}O_6Na^+$
			843.8	TAG (51:3) $C_{54}H_{99}O_6^+$ or $[TAG (49:0) + Na]^+$ $C_{52}H_{100}O_6Na^+$
			853.6	TAG (52:5) $C_{55}H_{97}O_6^+$ or $[TAG (50:2) + Na]^+$ $C_{53}H_{98}O_6Na^+$
			855.8	TAG (52:4) $C_{55}H_{99}O_6^+$ or $[TAG (50:1) + Na]^+$ $C_{53}H_{100}O_6Na^+$
unknown	438.5			
	440.6			
			533.4	
			535.4	
	552.4			
	554.6			
	556.6			
			561.5	
			589.6	
		720.5		
		722.5		

Many of the significant peaks detected from the fly brain with these different sample preparation methods, sublimation with DHB followed by matrix recrystallization with TFA, sublimation with CHCA, and modification with AuNPs, are listed in Table 1. It is clear that each method specifically detects different molecules although several of them, in particular, the lipids PC and PE can be observed using DHB and CHCA sublimation methods. Combining these protocols therefore can provide valuable complementary profiles of small metabolites, intact lipids, and lipid-related compounds in *Drosophila* brain. And, perhaps, these differences are general to all tissues.

DOI: 10.1021/acs.analchem.5b03942
Anal. Chem. 2016, 88, 1734−1741

CONCLUSIONS

The brain lipids of *Drosophila* have been profiled and imaged by MALDI and SALDI with a goal of comparing sample preparation via sublimation with organic matrix followed by recrystallization with TFA and surface modification with AuNPs. TFA is used to enhance the sensitivity of lipid imaging with DHB matrix; however, this has an insignificant effect on the CHCA matrix. Different sample preparation methods with a particular matrix material are specifically suitable for detection of different biomolecules including small molecules less than 400 Da, diacylglycerides, intact lipids, and triacylglycerides in the fly brains. Therefore, these different matrixes could be used in a complementary fashion to profile different aspects of the fly brain or other biological tissues. In addition, we show here that, for imaging of the fly brain at spatial resolution 20 μm, modification with AuNPs is superior when compared to sublimation with organic matrixes. The imaging protocol developed here provides the best and most diverse lipid chemical images of the fly brain to date.

ASSOCIATED CONTENT

Supporting Information

The Supporting Information is available free of charge on the ACS Publications website at DOI: 10.1021/acs.analchem.5b03942.

SEM images of distribution of gold NPs on a sample surface and on the surface of the fly brain, interferences of sample embedding materials on fly brain spectra, spectral interferences of DHB and CHCA at mass range below 400 Da, standard lipid DLPC and DOPC analyzed with matrixes DHB and CHCA, standard lipids on the fly brain analyzed using AuNP modification, spectra comparing MALDI and SALDI performances for fly brains obtained from different sample preparation methods, and list of enhanced peaks due to the use of TFA treatment after DHB sublimation (PDF)

AUTHOR INFORMATION

Corresponding Author

*E-mail: andrew.ewing@chem.gu.se.

Notes

The authors declare no competing financial interest.

ACKNOWLEDGMENTS

The authors acknowledge grants from The European Research Council (ERC), Knut and Alice Wallenberg Foundation, the Swedish Research Council (VR), and the National Institutes of Health.

REFERENCES

(1) Pandey, U. B.; Nichols, C. D. *Pharmacological Reviews.* **2011**, *63*, 411−436.
(2) Wolf, F. W.; Heberlein, U. *J. Neurobiol.* **2003**, *54*, 161−178.
(3) Kraut, R. *J. Neurochem.* **2011**, *116*, 764−778.
(4) Kliman, M.; Vijayakrishnan, N.; Wang, L.; Tapp, J. T.; Broadie, K.; McLean, J. A. *Mol. BioSyst.* **2010**, *6*, 958−966.
(5) Kaftan, F.; Vrkoslav, V.; Kynast, P.; Kulkarni, P.; Bocker, S.; Cvacka, J.; Knaden, M.; Svatos, A. *J. Mass Spectrom.* **2014**, *49*, 223−232.
(6) Urban, P. L.; Chang, C. H.; Wu, J. T.; Chen, Y. C. *Anal. Chem.* **2011**, *83*, 3918−3925.
(7) Phan, N. T.; Hanrieder, J.; Berglund, E. C.; Ewing, A. G. *Anal. Chem.* **2013**, *85*, 8448−8454.
(8) Phan, N. T.; Fletcher, J. S.; Ewing, A. G. *Anal. Chem.* **2015**, *87*, 4063−4071.
(9) Cillero-Pastor, B.; Heeren, R. M. *J. Proteome Res.* **2014**, *13*, 325−335.
(10) Thomas, A.; Chaurand, P. *Bioanalysis* **2014**, *6*, 967−982.
(11) Yang, J.; Caprioli, R. M. *Anal. Chem.* **2011**, *83*, 5728−5734.
(12) Poetsch, A.; Schlüsener, D.; Florizone, C.; Eltis, L.; Menzel, C.; Rögner, M.; Steinert, K.; Roth, U. *J. Biomol. Tech.* **2008**, *19*, 129−138.
(13) Bouschen, W.; Schulz, O.; Eikel, D.; Spengler, B. *Rapid Commun. Mass Spectrom.* **2010**, *24*, 355−364.
(14) Kaletas, B. K.; van der Wiel, I. M.; Stauber, J.; Dekker, L. J.; Guzel, C.; Kros, J. M.; Luider, T. M.; Heeren, R. M. *Proteomics* **2009**, *9*, 2622−2633.
(15) Chughtai, K.; Heeren, R. M. *Chem. Rev.* **2010**, *110*, 3237−3277.
(16) Goodwin, R. J. *J. Proteomics* **2012**, *75*, 4893−4911.
(17) Taira, S.; Sugiura, Y.; Moritake, S.; Shimma, S.; Ichiyanagi, Y.; Setou, M. *Anal. Chem.* **2008**, *80*, 4761−4766.
(18) Hayasaka, T.; Goto-Inoue, N.; Zaima, N.; Shrivas, K.; Kashiwagi, Y.; Yamamoto, M.; Nakamoto, M.; Setou, M. *J. Am. Soc. Mass Spectrom.* **2010**, *21*, 1446−1454.
(19) Gholipour, Y.; Giudicessi, S. L.; Nonami, H.; Erra-Balsells, R. *Anal. Chem.* **2010**, *82*, 5518−5526.
(20) Kong, X. L.; Huang, L. C. L.; Hsu, C. M.; Chen, W. H.; Han, C. C.; Chang, H. C. *Anal. Chem.* **2005**, *77*, 259−265.
(21) Agrawal, K.; Wu, H. F. *Rapid Commun. Mass Spectrom.* **2008**, *22*, 283−290.
(22) Wang, M. T.; Liu, M. H.; Wang, C. R.; Chang, S. Y. *J. Am. Soc. Mass Spectrom.* **2009**, *20*, 1925−1932.
(23) Chen, C. T.; Chen, Y. C. *Anal. Chem.* **2005**, *77*, 5912−5919.
(24) Su, C. L.; Tseng, W. L. *Anal. Chem.* **2007**, *79*, 1626−1633.
(25) Son, J.; Lee, G.; Cha, S. *J. Am. Soc. Mass Spectrom.* **2014**, *25*, 891−894.
(26) Goto-Inoue, N.; Hayasaka, T.; Zaima, N.; Kashiwagi, Y.; Yamamoto, M.; Nakamoto, M.; Setou, M. *J. Am. Soc. Mass Spectrom.* **2010**, *21*, 1940−1943.
(27) McLean, J. A.; Stumpo, K. A.; Russell, D. H. *J. Am. Chem. Soc.* **2005**, *127*, 5304−5305.
(28) Tanaka, K.; Waki, H.; Ido, Y.; Akita, S.; Yoshida, Y.; Yoshida, T.; Matsuo, T. *Rapid Commun. Mass Spectrom.* **1988**, *2*, 151−153.
(29) Huang, Y.-.; Chang, H.-T. *J. Mass Spectrom.* **2007**, *79*, 4852−4859.
(30) Roux, A.; Muller, L.; Jackson, S. N.; Baldwin, K.; Womack, V.; Pagiazitis, J. G.; O'Rourke, J. R.; Thanos, P. K.; Balaban, C.; Schultz, J. A.; Volkow, N. D.; Woods, A. S. *ACS Chem. Neurosci.* **2015**, *6*, 247−259.
(31) Jackson, S. N.; Baldwin, K.; Muller, L.; Womack, V. M.; Schultz, J. A.; Balaban, C.; Woods, A. S. *Anal. Bioanal. Chem.* **2014**, *406*, 1377−1386.
(32) Muller, L.; Kailas, A.; Jackson, S. N.; Roux, A.; Barbacci, D. C.; Schultz, J. A.; Balaban, C. D.; Woods, A. S. *Kidney Int.* **2015**, *88*, 186−192.
(33) Phan, N. T. N.; Fletcher, J. S.; Sjövall, P.; Ewing, A. G. *Surf. Interface Anal.* **2014**, *46*, 123−126.
(34) Kurczy, M. E.; Piehowski, P. D.; Parry, S. A.; Jiang, M.; Chen, G.; Ewing, A. G.; Winograd, N. *Appl. Surf. Sci.* **2008**, *255*, 1298−1304.
(35) Kimling, J.; Maier, M.; Okenve, B.; Kotaidis, V.; Ballot, H.; Plech, A. *J. Phys. Chem. B* **2006**, *110*, 15700−15707.
(36) Chughtai, K.; Jiang, L.; Greenwood, T. R.; Klinkert, I.; Amstalden van Hove, E. R.; Heeren, R. M.; Glunde, K. *Anal. Chem.* **2012**, *84*, 1817−1823.
(37) Weston, L. A.; Hummon, A. B. *Analyst* **2013**, *138*, 6380−6384.
(38) Yang, J.; Caprioli, R. M. *Anal. Chem.* **2011**, *83*, 5728−5734.

DOI: 10.1021/acs.analchem.5b03942
Anal. Chem. 2016, 88, 1734−1741